

Nonequilibrium Self-Assembly of Microtubules Through Stepwise Sequential Interactions of DNA

Jakia Jannat Keya, Mousumi Akter, Yuta Yamasaki, Yoshiyuki Kageyama, Kazuki Sada, Akinori Kuzuya,* and Akira Kakugo*

The assembly of biological systems forms nonequilibrium patterns with different functionalities through molecular-level communication via stepwise sequential interaction and activation. The mimicking of this molecular signaling offers extensive opportunities to design self-assemblies of bioinspired synthetic nonequilibrium systems to develop molecular robots with active, adaptive, and autonomous behavior. Herein, the design and construction of biomolecular motor system, microtubule (MT)-kinesin based molecular swarm system, are reported through stepwise sequential interactions of DNA. DNA signals are exchanged between three different DNA-tethered MTs, whereby the DNA signal from the first MT can activate the DNA strand on the second MT by communicating through physical contact, which facilitates assembly formation between the second and third DNA-tethered MTs. The DNA strands on the MTs can recognize the specific sequences of other DNA strands in the system and communicate with the complementary DNA on other MTs. This work will pave the way for developing autonomous molecular machines with advanced functionalities for complex nanotechnological applications.

active self-assembly.^[3,4] Passive self-assembly is driven by thermal energy and produces structures close to equilibrium in supramolecular systems or molecular crystals. Active self-assembly, in contrast, is driven by an applied energy source and produces nonequilibrium structures. In nature, a whole range of assemblies, from cellular proteins to biological microorganisms, is driven by molecular-level communication.^[5,6] Inspired by this, researchers have been working to understand molecular-level communication in order to trigger active self-assembly in synthetic systems with unprecedented levels of functionalities, e.g., adaptive and autonomous properties.^[7–11] Controlling active self-assembly in synthetic nonequilibrium systems through molecular-level communication may advance molecular machinery as well as nanotechnology.^[12–14] External energy, i.e., magnetic,^[15,16] electric,^[17,18] or light,^[19,20]

can power colloidal systems and permit the assembly formation, although this is not a self-propelled system. On the other hand, chemical,^[21] enzymatic,^[22] or photochemical reaction-driven^[23] self-propelled systems are utilized to demonstrate active self-assembly due to their active motion. Among enzymatic self-propelled systems, ATP-fueled biomolecular motor-driven cytoskeletal filaments^[4,24,25] have been extensively utilized to

1. Introduction

Self-assembly is the process in which individual components spontaneously organize into complex structures through their mutual communication or communication with the environment.^[1,2] From the viewpoint of thermodynamics, self-assembly can be divided into two classes, i.e., passive and

J. J. Keya
Department of Cell and Developmental Biology
University of Michigan Medical School
Ann Arbor, MI 48109, USA
M. Akter
Department of Mechanical Engineering
University of Michigan
Ann Arbor, MI 48108, USA

Y. Yamasaki, A. Kuzuya
Department of Chemistry and Materials Engineering
Kansai University
Osaka 564-8680, Japan
E-mail: kuzuya@kansai-u.ac.jp
Y. Kageyama, K. Sada
Graduate School of Chemical Sciences and Engineering
Hokkaido University
Sapporo 060-0810, Japan
K. Sada
Faculty of Science
Hokkaido University
Sapporo 060-0810, Japan
A. Kakugo
Department of Physics
Kyoto University
Kyoto 606-8224, Japan
E-mail: kakugo.akira.8n@kyoto-u.ac.jp

The ORCID identification number(s) for the author(s) of this article can be found under <https://doi.org/10.1002/smll.202408364>

© 2024 The Author(s). Small published by Wiley-VCH GmbH. This is an open access article under the terms of the [Creative Commons Attribution-NonCommercial-NoDerivs](#) License, which permits use and distribution in any medium, provided the original work is properly cited, the use is non-commercial and no modifications or adaptations are made.

DOI: 10.1002/smll.202408364

develop active self-assembly processes by controlling their interactions using associated proteins,^[26] depletion agents,^[27] ligand–receptor-based crosslinking,^[24,25,28] or DNA hybridization.^[29,30] The first three interactions lack programmability, but DNA can promote direct or stepwise sequential interactions that regulate assembly formation through molecular communication.^[31–37] Our group previously reported on DNA-assisted self-assembly of microtubules (MTs) driven by kinesin motors, where DNA was externally added to control the self-assembly process.^[29] Nevertheless, relying on external control limits the complexity of molecular communication needed for constructing active self-assembly systems.^[38] To address this challenge, we recently developed an autonomous, MT-based molecular machine in which DNA cascade reactions self-regulate the assembly of DNA-functionalized MTs without the need for external stimuli.^[30] However, this system depends on multiple enzymes and a DNA-based molecular control network for assembly initiation, with a centralized control mechanism sustaining the assembly and disassembly processes, rather than allowing independent, decentralized actions. Here we introduce an autonomous active self-assembly system in which DNA signals facilitate mutual communication between active agents, enabling a decentralized control mechanism. This approach is crucial as it eliminates the need for centralized enzymatic or molecular control, enhancing system adaptability and robustness. Learning the adaptability in the MT-kinesin system, DNA tethered to MTs can actively self-assemble the MTs through stepwise sequential interactions of DNA by transferring chemical messages. Specifically, one DNA-modified MT acts as a chemical messenger to activate a second DNA-modified MT, which then facilitates further active self-assembly with a third set of DNA-modified MTs. We also examine the kinetics of the DNA strand displacement reaction for message transfer and compare it to the MT-kinesin system. Our active self-assembly system offers advantages in achieving complex synchronized operations and adaptability in active matter systems and molecular machinery.^[39–41]

2. Results

The self-assembly formation of MTs through sequential interactions with DNA followed by activation is schematically illustrated in **Figure 1**. The system includes three different DNA-tethered MTs where MTs are modified with fluorescent dye-labeled DNA strands through a copper-free click reaction (**Figure 1a**). MTs modified with a complex of DNA strand 1 and DNA blocker (dS1/dB), DNA activator (dA), and DNA strand 2 (dS2) are assigned as green, blue, and red MTs, respectively. The sequences of DNA strands and their schematic representations are shown in **Figure 1b** (**Table S1**, Supporting Information). In the dS1/dB complex, yellow-colored dS1 hybridizes partially with pink blocker DNA strand, dB to give a bulge-loop structure in dS1. This structure protects the hybridization information (TTGTTGTTGTTG = TTG₄) with complementary DNA, dS2 (CAACAACAACAACA = CAA₅), in the red MT. At the 5'-end of dB, a 7 nucleotide protruding portion (TAAAGTG) is introduced to provide a toehold for sequence-selective strand displacement.^[42] Based on the melting temperature (T_m) simulation results, the base number in a DNA strand is fixed such that it works under ambient conditions (25 °C). To initiate hybridiza-

tion, blue activator DNA, dA, was designed as complementary to dB. Here, dA hybridizes with blocker DNA dB by a strand displacement reaction, and therefore free dS1 forms a duplex with a complementary dS2 strand in the next step. We confirmed the inhibition and initiation of the reactions between multiple DNA sequences through a non-denaturing polyacrylamide gel electrophoretic study (native PAGE) (**Figure 1c**). Native PAGE preserves the double-stranded structure of hybridized DNA, thereby ensuring that the mobility of the DNA is primarily determined by its length. The position of the DNA bands indicates whether two different DNA strands have formed an assembly. Lane dS1/dB indicates successful hybridization after annealing occurs between strands dS1 and dB, which is confirmed by the positions of the reference bands dS1, dB, and dS1+dB, which is a simple mixture of the two strands. The addition of dS2 did not change the band position, as observed from lane dS1/dB+dS2, which indicates complete inhibition of hybridization between dS1 and dS2 in the presence of dB. Further addition of the activator strand, dA, in the system initiated the strand displacement reaction of dB from dS1/dB. Thus, the duplex formation of dS1 and dS2 took place, as depicted from lanes dS1/dB+dS2+dA. The band positions from the reference bands indicate that the expected reaction between DNA strands occurred. This molecular recognition of DNA may facilitate the active self-assembly of dS1- and dS2-modified MTs followed by multistep displacement reactions as shown in **Figure 1d**.

Figure 2 demonstrates the active self-assembly of DNA-tethered MTs. In the presence of adenosine triphosphate (ATP), DNA-tethered MTs of 5–10 μm in length were observed to propel under fluorescence microscopy. The estimated velocity ($0.5 \pm 0.1 \mu\text{m s}^{-1}$; average \pm standard deviation, $n = 30$) of the MTs indicates that DNA conjugation does not hinder the interaction between MTs and kinesins. The total density ($70\,000 \text{ mm}^{-2}$) of the three MTs was adjusted to an $\approx 1:1:1$ ratio, and 0.3 μM recombinant kinesin, consisting of the first 573 amino acid residues of human kinesin-1, was used in the in vitro gliding assay experiment. We optimized the molarity concentration of tubulins and density of MTs in each experiment to maintain the density ratio of MTs. This optimized MT density was essential for achieving robust results in the MT assembly process. **Figure 2a** shows the fluorescence microscopy images of the self-assembly formation through the stepwise interaction of all three of the DNA-tethered MTs. The transfer of dB between the blue and green MTs might have occurred during their collision at 12 s after that they moved away. Then, the activated green MT collided with a red MT at 18 s at that point they began to move together. **Figure 2b** illustrates the possible interaction among three single MTs that expedited the assembly formation of red and green MTs. When a gliding dS1/dB-MT meets a dA-MT on the kinesin coated surface, we hypothesize that a minimum of one DNA strand displacement may be sufficient to enable subsequent interactions although direct evidence is lacking and further computational simulations are needed to explore these dynamics.

Next, the self-assembly of the DNA-tethered MTs was achieved through multistep DNA displacement reactions (**Figure 3**; **Movies S1–S4**, Supporting Information). The interactions of all four combinations of self-propelled MTs, (i) dS1/dB-MT + dS2-MT, (ii) dA-MT + dS2-MT, (iii) dS1/dB-MT + dA-MT, and (iv)

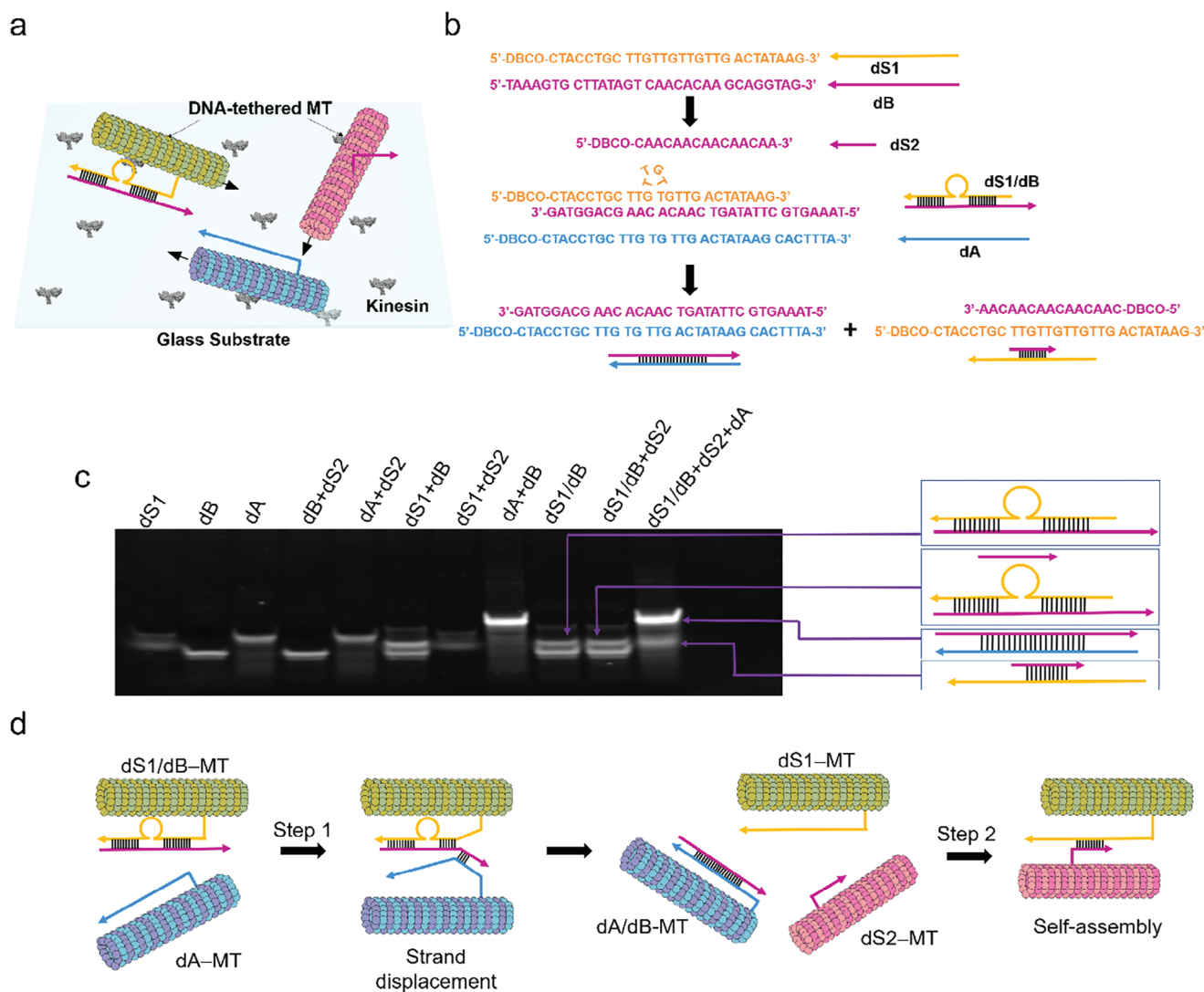


Figure 1. Schematic diagram of the stepwise sequential interaction of DNA and self-assembly of DNA-tethered MTs. a) Schematic illustration of the DNA-tethered MT gliding system on the kinesin-coated substrate. b) Sequences of DNA and their schematic representations in which dS1 is strand 1 for self-assembly (yellow-colored), dB is a blocker strand (pink-colored), dA is an activator strand (blue-colored), dS2 is strand 2 for self-assembly (pink-colored). c) Native PAGE analysis of the step-by-step transfer of the DNA signal (dB) through strand displacement reaction with dA. Lanes dS1, dB, dA, dB+dS2, dA+dS2, dS1+dB, and dA+dB show the reference bands corresponding to the DNA sequences. Lane dS1/dB shows the desired bulge DNA structure formation in the annealed system with a band corresponding to excess dB. Lane dS1/dB+dS2 shows no change in the band position after adding dS2 to the dS1/dB system, indicating the successful protection of the DNA strand. The final lane shows that dA triggers strand displacement and thus the formation of the dS1/dS2 complex. d) Schematic diagram of the self-assembly of MTs using stepwise signaling of DNA followed by DNA activation.

dS1/dB-MT + dA-MT + dS2-MT, were investigated (Figure 3a). Figure 3b shows time-lapse fluorescence microscopy images of the MT behaviors. As is indicated by the existence of the thick bundles in Figure 3b(iv), the self-assembly of the MTs was observed to occur in the presence of all of the DNA-tethered MTs. Lack of any one of the DNA-MTs resulted in individual MT movements without any association throughout the timeline (i-iii), indicating the AND-gated molecular recognition of the DNA sequence (Figure 3c). Self-assembly of the DNA-tethered MTs was quantitatively analyzed by counting the number of single MTs manually and dividing the number at time t by the initial num-

ber of MTs ($t = 0$) to produce an association ratio (Figure 3d). The association ratio increased over time and reached 86% after 60 min of ATP addition. The association ratios for other combinations did not change over time.

Finally, we studied the hybridization kinetics of the DNA reaction used for multistep signaling in solution and compared these kinetics with those of the active matter system (See Additional Sections S2, S3 and Figure S2, Supporting Information). The strand displacement reaction between dS1/dB and dA and the subsequent duplex formation between dS1 and dS2 were monitored by FRET quenching measurements of dS1 labeled with

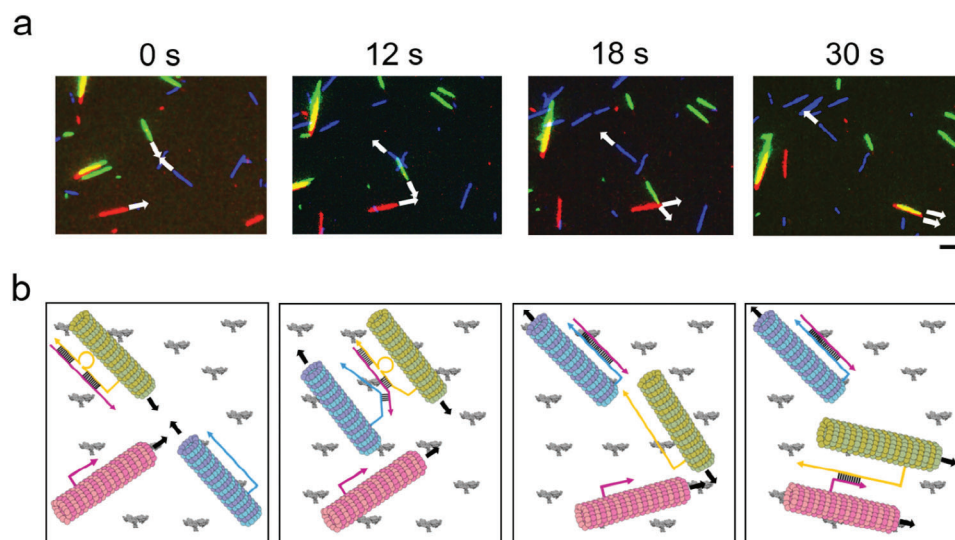


Figure 2. Visualization of stepwise sequential interaction of DNA through collisions between single DNA-tethered MTs. a) Time-lapse fluorescence microscopy images show the green and blue MTs approach each other, collide once (12 s), and separate (18 s). The green MT then communicates with a red MT through DNA hybridization at which point they begin to move together (30 s). Kinesin concentration: $0.3 \mu\text{M}$, scale bar: $5 \mu\text{m}$. b) Schematic illustration shows the possible interaction of DNA-tethered MTs after a collision, as observed in (a).

fluorescent dye in the bulk system. It was found that the rate constant of the second reaction was much faster than that of the first reaction ($k_1 = 0.7 \mu\text{M}^{-1} \text{min}^{-1}$ and $k_2 = 4.4 \mu\text{M}^{-1} \text{min}^{-1}$), indicating that the strand displacement reaction is the slowest, rate-limiting step. Compared to the bulk system, the reaction rate in the active matter system ($k = 0.2 \mu\text{M}^{-1} \text{min}^{-1}$) was much slower for hybridization of dS1 and dS2, which resulted in the self-assembly of dS1-MT and dS2-MT (Figure S3; Table S3, Supporting Information). In this case, the number of effective collisions of motile MTs is an important factor affecting the kinetics of the self-assembly of MTs. Similarly, we determined the rate of assembly formation in the presence of three DNA-tethered MTs in which self-assembly occurred by the multistep signaling of DNA. The rate constant was considerably slower ($k = 0.02 \mu\text{M}^{-1} \text{min}^{-1}$) than that of the dS1-MT and dS2-MT systems, indicating the contribution of the slowest step, i.e., the strand displacement reaction between dS1.dB-MT and dA-MT (Figure 4). The effect of the time of addition of dS2-MT on self-assembly formation was also studied by varying the time to 0, 10, and 30 min after the addition of ATP buffer to allow sufficient time for the interaction between dS1/dB-MT and dA-MT. Upon the addition of dS2-MT to the system, it was observed to react immediately with the free dS1-MTs (Figure 4a). The time-lapse fluorescence images reflect the time-dependent self-assembly formation considering the time of addition of dS2-MT to be 0 min. The change in the association ratio upon the addition of dS2-MT is presented in Figure 4b. The rate of self-assembly was found to increase almost double after the addition of dS2-MTs at 10 min ($k \approx 0.04 \mu\text{M}^{-1} \text{min}^{-1}$) and 30 min ($k \approx 0.04 \mu\text{M}^{-1} \text{min}^{-1}$) compared to 0 min (Figure 4c). The kinetics of self-assembly can be further tuned depending on the optimization of the velocity of the MTs, the number of effective collisions between them, surrounding macromolecular crowding, length of DNA strand, etc., which will be studied in our future research.

3. Discussions

This study addresses the conceptual and experimental challenges in achieving stepwise sequential interactions among DNA-modified biomolecular motors for the autonomous self-assembly of MTs within active matter systems. Specifically, we demonstrate that kinesin-driven MTs modified with DNA can communicate chemically, enabling autonomous signal transfer between MTs that facilitates higher-order self-assembly. Unlike previous approaches that relied on external molecular controls or enzymatic systems, this framework allows one DNA-modified MT to act as a molecular messenger that triggers subsequent interactions in a second, distinct population of MTs, which then catalyzes the assembly of a third set. This process represents a novel paradigm in active self-assembly, allowing MTs to interact sequentially and autonomously, thus overcoming prior limitations and enabling more sophisticated, multi-step assembly dynamics.

The key question of our study explores whether DNA-mediated communication between MTs enables a self-regulated, adaptive assembly system within active matter, by introducing a memory mechanism that allows MTs to dynamically change behavior in response to DNA signals and retain these modifications.^[30] This DNA-based memory facilitates not only the initiation and propagation of complex assembly sequences but also provides a foundation for adaptive, biomolecular motor-based systems with potential applications in tasks that require signal transduction, biosensing, and analytical applications.^[43–45]

Building on prior work that explored DNA-based assembly with external and enzymatic control, our approach is distinguished by its fully autonomous nature, wherein MTs can engage in multi-stage, self-propagating assembly without external intervention. This autonomy is crucial for developing scalable and resilient active matter systems that could eventually be deployed in

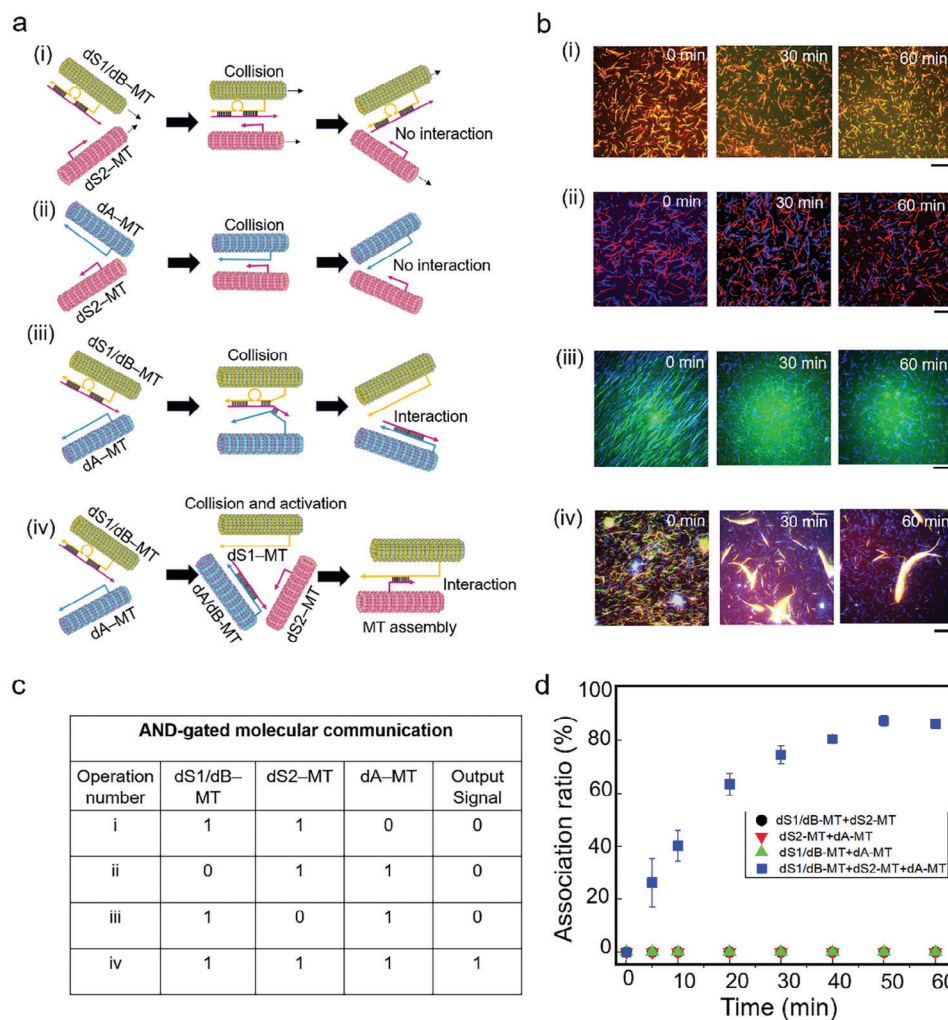


Figure 3. Assembly formation of different combinations of DNA-tethered MTs on kinesin-coated surfaces. i) dS1/dB-MT + dS2-MT, ii) dA-MT + dS2-MT, iii) dS1/dB-MT + dA-MT, and iv) dS1/dB-MT + dA-MT + dS2-MT. a) Schematic illustration of the interactions of the different combinations of DNA-tethered MTs (i), (ii), (iii), and (iv). b) Representative time-lapse fluorescence images of the DNA-tethered MTs in the different combinations (i), (ii), (iii), and (iv). Fluorescence microscopy images were taken after ATP addition to the solution. Kinesin concentration: 0.3 μM , scale bar: 20 μm . Number of trials: 3 c) Schematic table representing the AND-gated molecular communication of DNA which shows that all three DNA-tethered MTs are required for self-assembly. d) Time course of the association ratio of the self-assembly in the four combinations of self-propelled DNA-tethered MTs. Error bar: standard deviations. Statistical hypothesis testing was performed for association ratio of dS1/dB-MT+dS2-MT+dA-MT at 0, 30, and 60 min and the association ratio was found significantly different from 0 to 30, 30 to 60, and 0 to 60 min, having confidence intervals <0.001. The one-way and two-way ANOVA tests corrected with Tukey's Honest Significant Difference were used.

real-world environments requiring intricate operation and robust adaptability.^[46]

To introduce additional functionality and modularity, we explored approaches for enhancing the system's complexity and control. For example, the incorporation of secondary or bulge-loop DNA structures could facilitate hierarchical assembly pathways, enabling more sophisticated organization of MTs.^[47,48] Furthermore, by tethering small biomolecules (e.g., RNA, enzymes, antibodies) through DNA hybridization, we establish a versatile platform with significant potential for biosensing and analytical applications.^[49–52]

Further precise control of the reaction kinetics may be feasible since the properties of MTs, such as concentration (number), velocity change through ATP concentration, flexural rigid-

ity, or DNA density, can be freely and easily tunable. These tunable parameters allow us to precisely regulate reaction kinetics, creating highly controlled and programmable systems that outperform conventional solution-based mixtures.^[53] Incorporating photoresponsive molecules, such as azobenzene, into the DNA structure could further introduce reversibility and robust control in the self-assembly process.^[29,54]

In conclusion, our study contributes a significant advancement toward the realization of autonomous, biomolecular motor-based microscale machines. By embedding adaptive, self-regulating capabilities within MT assemblies, we set the stage for developing biomolecular systems capable of performing complex operations within active matter frameworks.^[14,41,55] Future work will focus on refining these control strategies and further

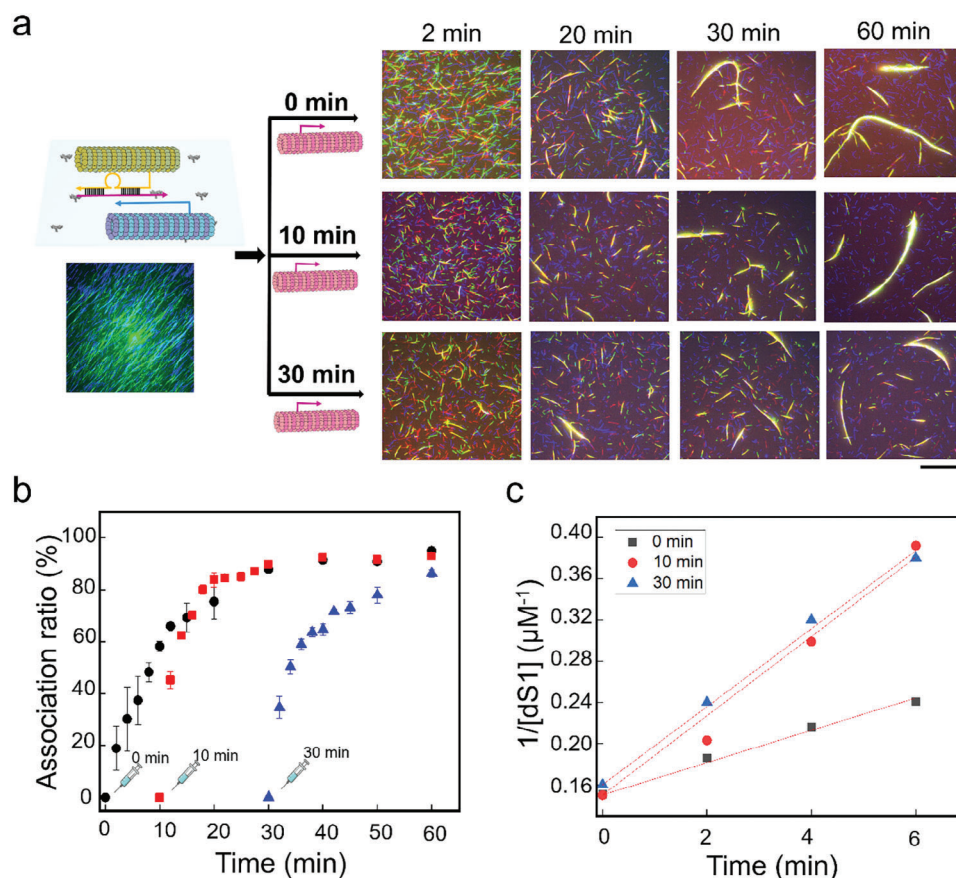


Figure 4. Kinetic control of MT self-assembly with the stepwise sequential interaction of DNA signals. a) Representative time-lapse fluorescence images of MT self-assembly with varying time upon dS2-MT addition at 0, 10, and 30 min after adding ATP buffer to the system to accelerate the kinetics. The time course of images reflects the time of self-assembly considering the addition of dS2-MT as 0 min. Scale bar: 20 μm. 3 repeats were performed. b) Time-dependent association ratio of the MT self-assembly upon time variation of dS2-MT addition at 0, 10, and 30 min after adding ATP buffer containing dS1.dB-MTs and dA-MTs. Error bars: standard deviations. c) Determination of the rate constant of hybridization of dS1 and dS2 resulting in MT self-assembly after adding dS2-MT to the system. The concentration of dS1 was determined from the estimated number of dS1 strands attached to single dS1-MTs with time. The estimated concentration of dS1 was fitted with the equation $(1/[dS_1-MT] = kt + 1/[dS_1-MT]_0)$ (details in [Supplementary Materials](#)) to estimate the rate constants for 0, 10, and 30 min addition as $k = 0.02, 0.04, \text{ and } 0.04 \mu\text{M}^{-1} \text{min}^{-1}$, respectively.

elucidating the system's potential for practical applications, while addressing remaining limitations in scalability and functional deployment in diverse environments.

4. Experimental Section

Design and Preparation of DNA Sequences: All the DNA strands were designed from simulation of melting temperature (T_m) using 'OligoAnalyzer 3.1' software with a T_m between 0 and 60 °C for experimental testing. Dibenzocyclooctyne (DBCO) and fluorescent dye-labeled strands were chemically synthesized using appropriate CPG columns and a phosphoramidite (Glen Research, VA) on an ABI 3900 automatic DNA synthesizer, purified by reverse phase HPLC and fully characterized by MALDI-TOF/MS (Bruker Microflex LRF). The DNA was modified at the 3' end with either ATTO-488, ATTO-550, or ATTO-647 and at the 5' end with DBCO. For DNA Native PAGE analysis, DNAs were purchased from Eurofins Genomics LLC, Hokkaido Science System (Japan), and Integrated DNA Technologies (IDT, Singapore).

Annealing of DNA Sequences: In order to prepare bulge DNA structures, DNA with the bulge sequence (dS1), and block DNA (dB) strands were annealed where the concentration ratio of bulge DNA: block DNA

was maintained as 1:2. The annealing was done by cooling the DNA solution at -0.5 °C per min from 95 to 25 °C using a thermal cycler (MiniAmp Plus).

Native PAGE Analysis of DNA Multi-Step Signaling: Native PAGE was used to separate and analyze shorter DNA while maintaining its double-stranded structure. The addition of a denaturant (i.e., urea) to the gel typically causes the DNA to become single-stranded. In denatured gels, secondary structures do not form, and as a result the mobility of the DNA was influenced solely by its length. 20% polyacrylamide gel was used to demonstrate the multi-step interaction of DNA signaling. 0.5 x TBE buffer (Tris base: 44.5 mM, Boric acid: 225 mM, EDTA: 1.275 mM, pH 8.3) was used as a running buffer and sample buffer with 8% glycerol. The gel was run on a WSE-1100 gel electrophoresis unit at 20 mA for 90 min at room temperature. Post-staining was done with 0.5 mgml⁻¹ gelstar and visualized by UV transillumination with ATTO-Luminograph.

Purification of Tubulin and Kinesin: Tubulin was purified from the porcine brain using a high-concentration PIPES buffer (1 M PIPES, 20 mM EGTA, and 10 mM MgCl₂) and stored in BRB80 buffer (80 mM PIPES, 1 mM EGTA, 2 mM MgCl₂, pH adjusted to 6.8 using KOH).^[56] In brief, food-grade porcine brains were purchased from a local slaughterhouse, and conserved before use in ice-cold PBS (phosphate buffer saline) prepared by mixing 137 mM NaCl, 8.1 mM Na₂HPO₄, 2.68 mM KOH and

1.47 mM KH₂PO₄ (all reagents from WAKO Pure Chemical Corporation, Japan). High-concentration PIPES buffer and Brinkley BR buffer 1980 (BRB80) were prepared using the dipotassium salt of PIPES (Sigma-Aldrich, USA), and the pH was adjusted to 6.8 using KOH (WAKO Pure Chemical Corporation, Japan). Recombinant kinesin-1 consisting of the first 573 amino-acid residues of human kinesin-1 was prepared as described in the literature.^[57] Azide-labeled tubulin was prepared using N₃-PEG4-NHS following the established protocol of labeling tubulin with a fluorescent dye.^[56,58] The tubulin concentration was determined by measuring the absorbance at 280 nm using a UV spectrophotometer (Nanodrop 2000c).

Preparation of MTs with DNA Sequences: MTs were prepared by adding azide tubulin to polymerization buffer (80 mM PIPES, 1 mM EGTA, 1 mM MgCl₂, 1 mM polymerizing agent, pH 6.8) in a 4:1 ratio, where the final concentration of tubulin was 56 μM incubating at 37 °C for 30 min. The polymerizing agent was Guanosine-5'-[(α,β)-methylene]triphosphate (GMPCPP), a slowly hydrolyzable analog of guanosine triphosphate (GTP) to prepare short and rigid MTs. Copper-free click reaction was initiated by adding 3.5 μL DBCO conjugated DNAs (≈500 μM) to the 5 μL azide-MTs (56 μM), which allowed azide-alkyne cycloaddition reaction and incubated at 37 °C for 6 h.^[59] 100 μL of cushion buffer (BRB80 buffer supplemented with 60% glycerol) was used to separate the MTs by centrifugation at 201000 × g (S55A2-0156 rotor, Hitachi) for 1 h at 37 °C. After removing the supernatant, the pellet of DNA-conjugated MTs was washed once with 100 μL BRB80P (BRB80 supplemented with 1 mM taxol) and dissolved in 15 μL BRB80P.

Demonstration of Self-Assembly of MTs Using Stepwise Signaling of DNA: A flow cell with dimensions of 9 × 2.5 × 0.1 mm³ (L × W × H) was assembled from two cover glasses (MATSUNAMI Inc.) using a double-sided tape as a spacer. The flow cell was filled with 5 μL casein buffer (BRB80 buffer supplemented with 0.5 mg mL⁻¹ casein). After incubating for 3 min, 0.3 μM kinesin solution was introduced into the flow cell and incubated for 5 min resulting in a density of 4000 μm⁻² on the substrate. Kinesin density for different feed concentrations was estimated using quartz crystal microbalance following this previous report.^[60] After washing the flow cell with 5 μL of wash buffer (BRB80 buffer supplemented with 1 mM DTT, 10 μM taxol), 5 μL of green dS1/dB-MTs solution was introduced and incubated for 2 min, followed by washing with 10 μL of wash buffer. Subsequently, 5 μL of the red dS2-MTs solution was introduced and incubated for 2 min, followed by washing with 10 μL of motility buffer. Then finally 5 μL of blue dA-MTs was introduced and incubated for 2 min, followed by washing with 10 μL of motility buffer. The motility of MTs was initiated by applying 5 μL ATP buffer (wash buffer supplemented with 5 mM ATP, 4.5 mg mL⁻¹ D-glucose, 50 U mL⁻¹ glucose oxidase, 50 U mL⁻¹ catalase, and 0.2% methylcellulose (w/v)). The wash buffer and ATP buffer contain 1 mM of MgCl₂. The ATP buffer, containing 5 mM ATP and 1 mM Mg²⁺, ensures that the available 1 mM Mg²⁺ preferentially forms 1 mM Mg-ATP complexes,^[61,62] which were adequate for activating kinesins and facilitating its binding to MTs, as well as supporting motility. The excess ATP remaining in the solution as free ATP does not interfere with kinesin activity. The time of ATP addition was set as 0 h. Soon after the addition of ATP buffer, the flow cell was placed in an inert chamber system (ICS)^[63] and the MTs were monitored using a microscope at room temperature (25 °C). The experiment was performed at least 3 times for each condition. The samples were illuminated with a 100 W mercury lamp and visualized by an epifluorescence microscope (Eclipse Ti, Nikon) using an oil-coupled Plan Apo 60× N.A.1.4 objective (Nikon). UV cut-off filter blocks (TRITC: EX 540/25, DM565, BA605/55; GFP-B: EX460-500, DM505, BA510-560; Cy5: EX 604/644, DM660, EM 672/712 Nikon) were used in the optical path of the microscope. Images were captured using a cooled-CMOS camera (NEO sCMOS, Andor) connected to a PC. Two ND filters (ND4, 25% transmittance for TRITC and ND2, 50% transmittance for GFP-B and Cy5) were inserted into the illumination light path of the fluorescence microscope to reduce photobleaching of the samples.

Estimation of the Association Ratio of MTs: The time-dependent association ratio $R(t)$ of red and green MTs was determined by counting the

number of single MTs manually and dividing the number at time t by the number present initially ($t = 0$) as follows

$$R(t) = \left(\frac{N(0) - N(t)}{N(0)} \right) \quad (1)$$

with $N(0)$ = Initial number of single MTs, $N(t)$ = Number of single MTs after time t . The mean association ratio was obtained from the average of four regions of interest (138.5 μm × 117 μm).

Statistical Analysis: All statistical analyses were performed using NIS-Elements software (Nikon Instruments Inc.) and Image J software (ij152-win-java8, Center for Information Technology, Bethesda, Maryland, USA). The analyzed data were plotted using OriginPro19 software (OriginPro version 2019, OriginLab Corporation, Northampton, MA, USA). Statistical analyses were performed using GraphPad Prism. The one-way and two-way ANOVA tests corrected with Tukey's Honest Significant Difference were used.

Supporting Information

Supporting Information is available from the Wiley Online Library or from the author.

Acknowledgements

J.J.K. and M.A. contributed equally to this work. This work was financially supported by the Grants-in-Aid for Scientific Research on Innovative Areas "Molecular Robotics" (JSPS KAKENHI Grant Number JP24104004), "Molecular Engine" (No. 18H05423 and 19H05407), the Scientific Research (A) (Grant No. 18H03673), Grant-in-Aid for Transformative Research Areas (Grant No. 20H05972) and Challenging Research (Pioneering) (19K22261) from the Japan Society for the Promotion of Science (JSPS). The authors also acknowledge the support from the Future AI and the Robot Technology Research and Development Project from New Energy and Industrial Technology Development Organization (NEDO), Japan.

Conflict of Interest

The authors declare no conflict of interest.

Author Contributions

J.J.K., A.Ka., A.Ku., and M.A. conceptualized the study. J.J.K. curated the data. J.J.K. and Y.K. performed formal analysis. M.A. performed supporting analysis. J.J.K. performed investigations. J.J.K. and Y.Y. performed the methodology. J.J.K., A.Ka., A.Ku., and K.S. performed validation. J.J.K., A.Ka., A.Ku., and M.A. wrote the original draft of the manuscript. J.J.K., M.A., A.Ka., and A.Ku. reviewed and edited the final manuscript.

Data Availability Statement

The data that support the findings of this study are available from the corresponding author upon reasonable request.

Keywords

biomolecular motor system, DNA, microtubule-kinesin, self-assembly, stepwise sequential interaction

Received: September 13, 2024

Revised: December 5, 2024

Published online:

- [1] G. M. Whitesides, B. Grzybowski, *Science* **2002**, 295, 2418.
- [2] G. M. Whitesides, M. Boncheva, *Proc. Natl. Acad. Sci.* **2002**, 99, 4769.
- [3] V. VanDelinder, S. Brener, G. D. Bachand, *Biomacromolecules* **2016**, 17, 1048.
- [4] A. T. Lam, V. VanDelinder, A. M. R. Kabir, H. Hess, G. D. Bachand, A. Kakugo, *Soft Matter* **2016**, 12, 988.
- [5] D. Philp, J. F. Stoddart, *Angew. Chem. Int. Ed. Eng.* **1996**, 35, 1154.
- [6] A. C. Mendes, E. T. Baran, R. L. Reis, H. S. Azevedo, *Wiley Interdiscip. Rev.: Nanomed. Nanobiotechnol.* **2013**, 5, 582.
- [7] J. Dong, C. Zhou, Q. Wang, *Top. Curr. Chem.* **2020**, 378, 33.
- [8] L. N. Green, H. K. K. Subramanian, V. Mardanlou, J. Kim, R. F. Hariadi, E. Franco, *Nat. Chem.* **2019**, 11, 510.
- [9] R. Merindol, A. Walther, *Chem. Soc. Rev.* **2017**, 46, 5588.
- [10] W. Wang, W. Duan, S. Ahmed, A. Sen, T. E. Mallouk, *Acc. Chem. Res.* **2015**, 48, 1938.
- [11] M. Rubenstein, A. Cornejo, R. Nagpal, *Science* **2014**, 345, 795.
- [12] S. Chowdhury, W. Jing, D. J. Cappelleri, *J. Microbio Robot.* **2015**, 10, 1.
- [13] A. V. Pinheiro, D. Han, W. M. Shih, H. Yan, *Nat. Nanotechnol.* **2011**, 6, 763.
- [14] H. Wang, M. Pumera, *Chem. Soc. Rev.* **2020**, 49, 3211.
- [15] H. Xie, M. Sun, X. Fan, Z. Lin, W. Chen, L. Wang, L. Dong, Q. He, *Sci. Robot.* **2019**, 4, eaav8006.
- [16] A. Snezhko, I. S. Aranson, *Nat. Mater.* **2011**, 10, 698.
- [17] M. E. Leunissen, H. R. Vutukuri, A. Van Blaaderen, *Adv. Mater.* **2009**, 21, 3116.
- [18] A. Van Blaaderen, M. Dijkstra, R. van Roij, A. Imhof, M. Kamp, B. W. Kwaadgras, T. Vissers, B. Liu, *Eur. Phys. J. Spec. Top.* **2013**, 222, 2895.
- [19] J. Palacci, S. Sacanna, A. P. Steinberg, D. J. Pine, P. M. Chaikin, *Science* **2013**, 339, 936.
- [20] F. Schmidt, B. Liebchen, H. Löwen, G. Volpe, *J. Chem. Phys.* **2019**, 150, 94905.
- [21] S. De, R. Klajn, *Adv. Mater.* **2018**, 30, 1706750.
- [22] A. C. Hortelao, C. Simó, M. Guix, S. Guallar-Garrido, E. Julián, D. Vilela, L. Rejc, P. Ramos-Cabrer, U. Cossío, V. Gómez-Vallejo, T. Patiño, J. Llop, S. Sánchez, *Sci. Robot.* **2021**, 6, eabd2823.
- [23] B. Dai, J. Wang, Z. Xiong, X. Zhan, W. Dai, C. C. Li, S. P. Feng, J. Tang, *Nat. Nanotechnol.* **2016**, 11, 1087.
- [24] H. Hess, J. Clemmens, C. Brunner, R. Doot, S. Luna, K. H. Ernst, V. Vogel, *Nano Lett.* **2005**, 5, 629.
- [25] Y. Tamura, R. Kawamura, K. Shikinaka, A. Kakugo, Y. Osada, J. P. Gong, H. Mayama, *Soft Matter* **2011**, 7, 5654.
- [26] V. Schaller, K. M. Schmoller, E. Karaköse, B. Hammerich, M. Maier, A. R. Bausch, *Soft Matter* **2013**, 9, 7229.
- [27] D. Inoue, G. Gutmann, T. Nitta, A. M. R. Kabir, A. Konagaya, K. Tokuraku, K. Sada, H. Hess, A. Kakugo, *ACS Nano* **2019**, 13, 12452.
- [28] S. Kumar, G. Milani, H. Takatsuki, T. Lana, M. Persson, C. Frasson, G. Te Kronnie, A. Månsson, *Analyst* **2016**, 141, 836.
- [29] J. J. Keya, R. Suzuki, A. M. R. Kabir, D. Inoue, H. Asanuma, K. Sada, H. Hess, A. Kuzuya, A. Kakugo, *Nat. Commun.* **2018**, 9, 453.
- [30] I. Kawamata, K. Nishiyama, D. Matsumoto, S. Ichiseki, J. J. Keya, K. Okuyama, M. Ichikawa, A. M. d. R. Kabir, Y. Sato, D. Inoue, S. Murata, K. Sada, A. Kakugo, S.-I. M. Nomura, *Sci. Adv.* **2024**, 10, eadn4490.
- [31] L. Heinen, A. Walther, *Sci. Adv.* **2019**, 5, eaaw0590.
- [32] L. Qian, E. Winfree, *Science* **2011**, 332, 1196.
- [33] J. Fern, R. Schulman, *Nat. Commun.* **2018**, 9, 3766.
- [34] P. L. Biancanello, A. J. Kim, J. C. Crocker, *Phys. Rev. Lett.* **2005**, 94, 58302.
- [35] Y. Zhang, A. McMullen, L.-L. Pontani, X. He, R. Sha, N. C. Seeman, J. Brujic, P. M. Chaikin, *Nat. Commun.* **2017**, 8, 21.
- [36] G. Gines, A. S. Zadorin, J.-C. Galas, T. Fujii, A. Estevez-Torres, Y. Rondelez, *Nat. Nanotechnol.* **2017**, 12, 351.
- [37] A. Kuzyk, R. Schreiber, Z. Fan, G. Pardatscher, E.-M. Roller, A. Högele, F. C. Simmel, A. O. Govorov, T. Liedl, *Nature* **2012**, 483, 311.
- [38] J. Deng, A. Walther, *Nat. Commun.* **2020**, 11, 3658.
- [39] M. Hagiya, A. Konagaya, S. Kobayashi, H. Saito, S. Murata, *Acc. Chem. Res.* **2014**, 47, 1681.
- [40] M. Akter, J. J. Keya, K. Kayano, A. M. R. Kabir, D. Inoue, H. Hess, K. Sada, A. Kuzuya, H. Asanuma, A. Kakugo, *Sci. Robot.* **2022**, 7, eabm0677.
- [41] A. R. Kabir, D. Inoue, A. Kakugo, *Sci. Technol. Adv. Mater.* **2020**, 21, 323.
- [42] P. Stömmmer, H. Kiefer, E. Kopperger, M. N. Honemann, M. Kube, F. C. Simmel, R. R. Netz, H. Dietz, *Nat. Commun.* **2021**, 12, 4393.
- [43] L. Zhang, V. Marcos, D. A. Leigh, *Proc. Natl. Acad. Sci.* **2018**, 115, 9397.
- [44] F. Lancia, A. Ryabchun, N. Katsonis, *Nat. Rev. Chem.* **2019**, 3, 536.
- [45] I. Arahamian, *ACS Cent. Sci.* **2020**, 6, 347.
- [46] G. Volpe, N. A. Araújo, M. Guix, M. Miodownik, N. Martin, L. Alvarez, J. Simmchen, R. Di Leonardo, N. Pellicciotta, Q. Martinet, J. Palacci, *arXiv preprint arXiv* **2024**, 2407, 10623.
- [47] W. M. Jacobs, D. Frenkel, *J. Am. Chem. Soc.* **2016**, 138, 2457.
- [48] Y. Dong, C. Yao, Y. Zhu, L. Yang, D. Luo, D. Yang, *Chem. Rev.* **2020**, 120, 9420.
- [49] J. Zhai, H. Cui, R. Yang, *Biotechnol. Adv.* **1997**, 15, 43.
- [50] S. W. Dutse, N. A. Yusof, *Sensors* **2011**, 11, 5754.
- [51] J. Huang, S. Gambietz, B. Saccà, *Small* **2023**, 19, 2202253.
- [52] C. Ma, S. Li, Y. Zeng, Y. Lyu, *Biosensors* **2024**, 14, 236.
- [53] D. Soloveichik, G. Seelig, E. Winfree, *Proc. Natl. Acad. Sci.* **2010**, 107, 5393.
- [54] M. Akter, A. M. R. Kabir, J. J. Keya, K. Sada, H. Asanuma, A. Kakugo, *ACS Omega* **2024**, 9, 37748.
- [55] G. Saper, H. Hess, *Chem. Rev.* **2020**, 120, 288.
- [56] S. Ishii, M. Akter, J. J. Keya, M. R. Rashid, F. Afroze, S. R. Nasrin, A. Kakugo, *Purification of Tubulin from Porcine Brain and its Fluorescence Dye Modification. Microtubules. Methods in Molecular Biology*, Vol. 2430, (Eds.: H. Inaba), Humana, New York, NY **2022**, pp. 3–16.
- [57] R. B. Case, D. W. Pierce, *Cell* **1997**, 90, 959.
- [58] J. Peloquin, Y. Komarova, G. Borisy, *Nat. Methods* **2005**, 2, 299.
- [59] M. Akter, J. J. Keya, A. M. R. Kabir, H. Asanuma, K. Murayama, K. Sada, A. Kakugo, *Chem. Commun.* **2020**, 56, 7953.
- [60] A. M. d. R. Kabir, D. Inoue, T. Afrin, H. Mayama, K. Sada, A. Kakugo, *Sci. Rep.* **2015**, 5, 17222.
- [61] J. C. Cochran, T. C. Krzysiak, S. P. Gilbert, *Biochemistry* **2006**, 45, 12334.
- [62] J. Q. Cheng, W. Jiang, D. D. Hackney, *Biochemistry* **1998**, 37, 5288.
- [63] A. M. R. Kabir, D. Inoue, A. Kakugo, A. Kamei, J. P. Gong, *Langmuir* **2011**, 27, 13659.